

Parameters Limiting Sulfation by CaO

G. A. Simons

Physical Sciences Inc.
Andover, MA 01810

In situ sulfur removal from coal-fired boilers has been accomplished with reasonable success (Drehmel 1983; Drehmel et al., 1983). Either calcium carbonate or calcium hydroxide is injected into the post-flame combustion region, where it decomposes into CaO and reacts with SO₂ to form a calcium sulfate product. The sulfation rates and sorbent utilizations have been shown to be strong functions of the furnace temperature, quench rates, and of the sorbent size and internal surface area. However, the precise trade-offs between the controlling parameters have not been explicitly determined. Some theoretical guidelines are necessary to isolate the rate-controlling parameters.

A sorbent model that describes SO₂ retention by porous CaO has been developed (Simons and Garman, 1986) and verified (Simons et al., 1987). The mechanistic description of the process includes the pore structure, pore branching, species transport, reaction kinetics, product deposition, pore filling, pore plugging, and diffusion through the product layer. Small-pore filling is dominant for 1 to 10 μm dia. particles, while pore-mouth plugging is dominant for 100 μm to 1 mm dia. particles. Rate limitations due to product layer diffusion (prior to plugging or filling) are more pronounced for the thicker product layers occurring within the larger pores of the larger particles.

The process of small-pore filling and the associated internal surface area reduction has been validated from the BET adsorption data of Roman et al. (1984; see Simons and Garman, 1986). The sulfation rate on small particles (1 to 10 μm) is kinetically controlled on a time-varying surface area by an intrinsic rate constant that is first order in SO₂ pressure. The combined effects of pore filling and a first-order intrinsic rate constant yield a utilization vs. SO₂ curve that suggests an apparent reaction order that is fractional in SO₂ concentration. This is illustrated in Figure 1. Within a fixed reaction time, an increase in the SO₂ pressure will result in a greater degree of pore filling and surface area reduction. Hence, the faster intrinsic kinetics will react on a smaller internal surface area. The result is an apparent fractional reaction order that is a function of sorbent porosity, surface area, size, utilization, and SO₂ background pressure. It is emphasized here that the model depicts that there is no single scaling law, only qualitative trends.

The model has been validated with sulfation data on a wide range of particle diameters (1 μm to 1 mm), SO₂ partial pres-

ures (60 Pa to 5 kPa) and temperatures (973 to 1,478 K). Below, the model is used to examine the dominating effects of the reaction temperature and quench rate on sulfation. It is also used to illuminate the important role of sorbent size, porosity, and surface area on the sulfation rate. The effect of pore size distribution has been examined (Simons, 1987) and it is shown that tailoring the pore structure (with porosity and surface area constant) does not significantly enhance the sulfation process. Sorbent utilization may best be enhanced by a proper balance of particle size, porosity, surface area, and particle time-temperature history. The explicit effect of each variable is illustrated below.

Temperature Dependence of Sulfation in the Absence of Sintering

The intrinsic rate constant (Simons et al., 1987) expresses the kg of SO₂ reacted per second per m² internal surface area per MPa SO₂ partial pressure in an oxygen environment of 4 kPa.

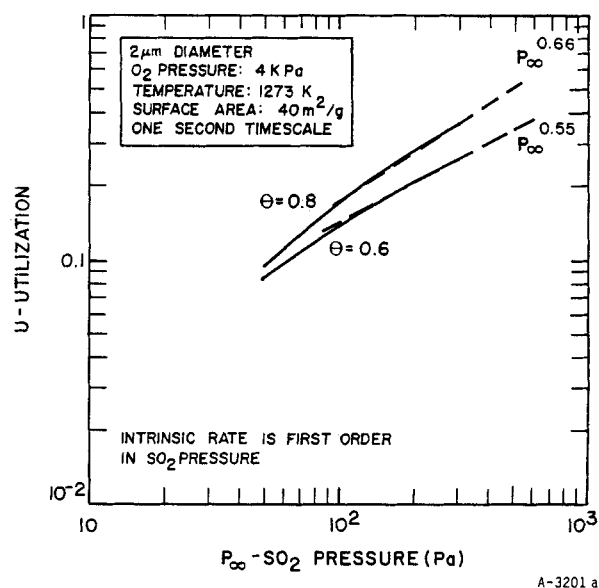


Figure 1. SO₂ pressure dependence.

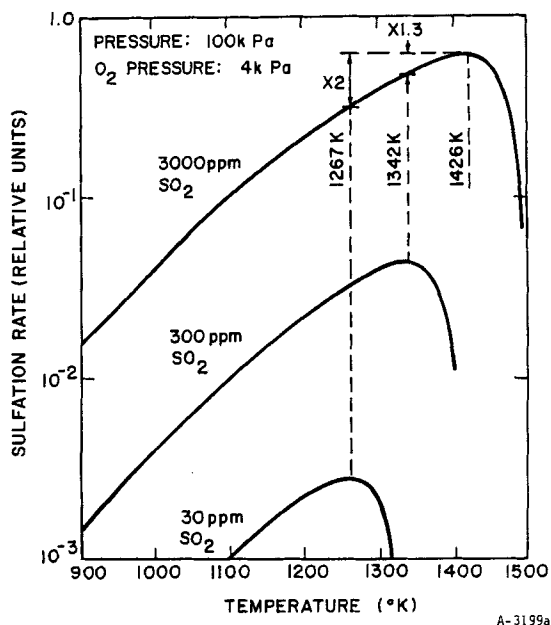


Figure 2. Intrinsic SO₂ sorption rate.

The value of k_s is expressed as

$$k_s = A \exp(-E/T) \quad (1)$$

where $A = 6 \times 10^4 \text{ kg/m}^2 \cdot \text{s} \cdot \text{MPa}$ and $E = 17,000 \text{ K}$.

At elevated temperature, there is a decrease in the net SO₂ sorption rate because of the decomposition of the CaSO₄ product. This backward reaction occurs at elevated temperature when the equilibrium vapor pressure p_v of the SO₂ approaches the partial pressure of the SO₂, p_s . This decrease in the net SO₂ conversion rate to the CaSO₄ product is accounted for by adjustment of the intrinsic rate constant according to

$$k'_s = k_s (1 - p_v/p_s) \quad (2)$$

where p_v is given by

$$p_v = A_2 \exp(-E_2/T) \quad (3)$$

and E_2 is approximately 52,000 K. The preexponential factor A_2 is given by

$$A_2 = 10^{12} / (p_{O_2})^{1/2} \text{ MPa} \quad (4)$$

where p_{O_2} is the oxygen partial pressure in kPa. For an oxygen partial pressure of 4 kPa and an SO₂ partial pressure of 300 Pa, CaSO₄ is unstable above 1,484 K.

Although the sulfate is stable below 1,484 K, the net sulfation rate is retarded due to the back reaction. The maximum rate of SO₂ conversion occurs when $dk_s/dT = 0$, which readily converts to

$$T_{opt} = \frac{E_2}{\ln [(A_2/p_s)(1 + E_2/E)]} \quad (5)$$

or 1,426 K for the conditions corresponding to sulfate instability above 1,484 K. The temperature dependence of the sulfation

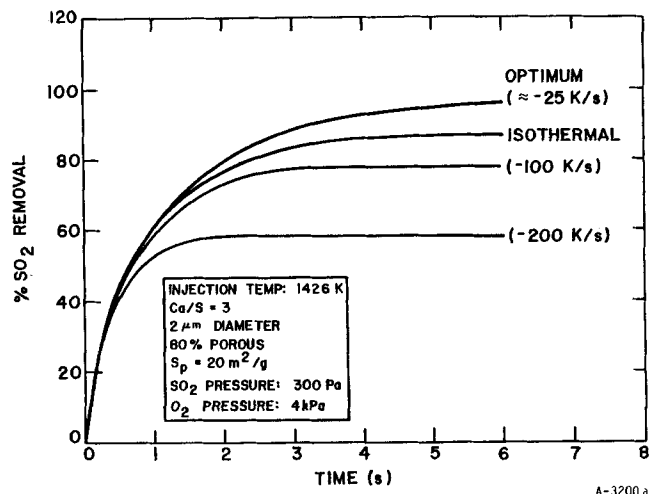


Figure 3. Effect of quench rate on SO₂ removal in the absence of sintering.

rate is illustrated in Figure 2. Note that while the optimum sulfation rate in typical atmospheric combustors occurs near 1,400 K, one may never achieve 90% removal (300 ppm) at 1,400 K because the sulfate is unstable under these conditions. The optimum temperature for 300 ppm is 1,342 K, but operation at 1,342 K over all SO₂ pressures would result in a 30% loss in the rate at the inlet (3,000 ppm). Injection at the higher temperature followed by mild quenching is required. In actual boiler applications, injection at a high post-flame temperature followed by quenching is the preferred mode of sorbent injection. Clearly quenching from 1,426 to 1,342 K (for 90% removal) will optimize the rates and minimize the required calcium.

The optimum quenching rates are specified by $T_{opt}(p_s)$ where $p_s(t)$ is the sulfur partial pressure as measured in flow time t after injection. These quenching rates are extremely sensitive to the particle surface area, porosity, and/or Ca/S ratio. Typical optimum quench rates are not linear but will vary from -25 to -100 K/s. Quench rates in typical American boilers are somewhat higher than this.

An example of SO₂ removal obtained for various quenching

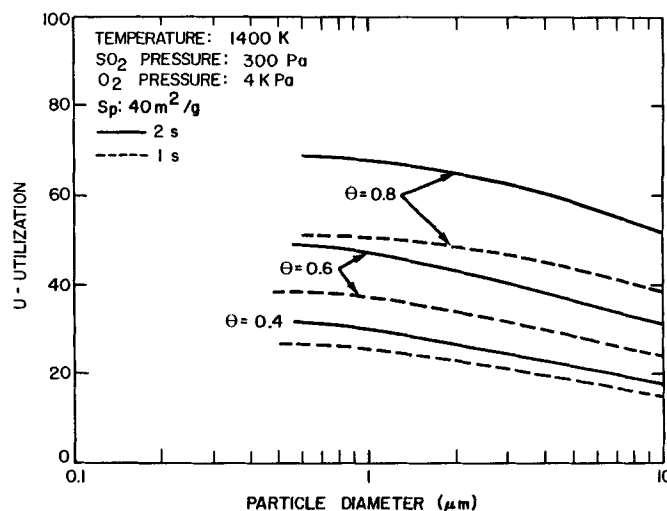


Figure 4. Effect of particle size and porosity on utilization.

rates is illustrated in Figure 3. The isothermal case yielded approximately 85% removal before equilibrium prevented additional sulfate from forming. Quenching at 100 to 200 K/s was much too fast and kinetic activity was lost. The optimum quench rate (≈ -25 K/s) yielded approximately 90% removal in 3 s and 95% in 5 s. Hence, proper quenching can increase the SO_2 removal but if quenching is carried out randomly, it may also be detrimental.

This study is based on kinetics alone, as neither calcination/dehydration of the sorbent nor sintering has been considered. Since sintering can be appreciable above 1,250 K, one may wish to quench faster or operate cooler. The trade-off between enhanced kinetics and sintering rates are beyond the scope of this study, but all empirical evidence and modeling results suggest that the trade-off occurs between 1,250 and 1,450 K. Attempting sulfation in an atmospheric combustor above 1,450 K would yield no apparent advantages. Pressurized combustors may be sulfated at higher temperatures if sintering is not detrimental (1,520 K at 1 MPa and 3,000 ppm SO_2).

Variation of Sulfation Rates with Porosity and Surface Area

A wide variety of sulfation data demonstrate a sensitivity of sulfation rates to particle size, SO_2 pressure, and sorbent type. The pore plugging/filling model of Simons and Garman (1986) has explained this database from the viewpoint that the SO_2 pressure and the sorbent size, porosity, and surface area are the only relevant variables and that all CaO is chemically the same, regardless of the carbonate or hydrate from which it was derived. In addition, particle-size dependence may be either explicit or implicit. That is, the particle size may directly affect sulfation or it may control the surface area and porosity that evolve during calcination or hydration of the raw material. The parametric study presented below seeks to illuminate the relative roles of these parameters and suggest test series on the basis of the theoretical predictions.

The roles of particle size and porosity are illustrated in Figure 4. The surface area, gas composition, temperature, and reaction time are fixed at the indicated values. Note that particle poros-

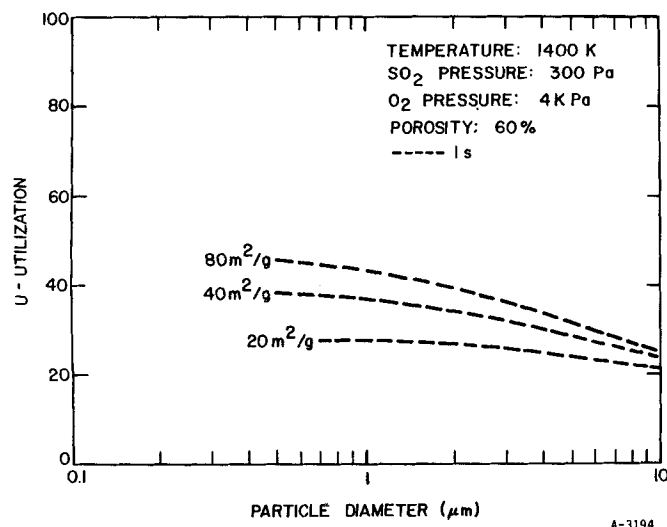


Figure 5. Effect of particle size and surface area on utilization.

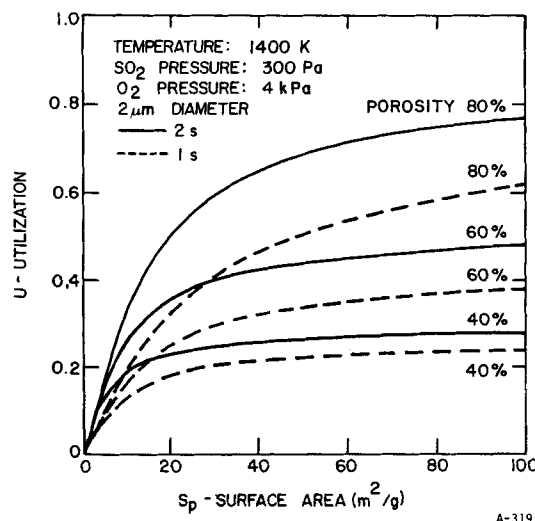


Figure 6. Effect of surface area and porosity on utilization at 300 Pa SO_2 .

ity controls sorbent utilization to a much greater extent than does particle size in the range indicated. Hence, any effect of particle size on porosity (during calcination) will have a greater implicit effect on sulfation than will the explicit effect of size. A similar trend with surface area is illustrated in Figure 5. Both surface area and porosity will enhance utilization. The trade-off between porosity and surface area at fixed particle size is illustrated in Figure 6. For any given porosity and reaction duration, utilization asymptotes with S_p . This is due to the fact that higher surface area is generated in smaller pores, which fill very fast. Alternatively, if the same S_p were contained in a higher porosity sorbent, the size of the smallest pore would be greater and pore filling would not occur as rapidly. These calculations suggest that a 40 m^2/g sorbent cannot be improved upon unless porosity is increased. This may be accomplished either through a yet to be determined calcination process or by choosing a high (15%) porosity carbonate or hydrate from which to derive the calcine. In much of the work to date, little attention has been paid to the role of porosity in determining the sulfation rates. In future tests, it is suggested that the porosity be measured and used as a correlation parameter.

Conclusions

A validated computer model has been used to demonstrate that the four most important parameters that can be used to enhance sulfation are the SO_2 pressure, optimum temperature for maintaining equilibrium, sorbent surface area (after calcination), and sorbent porosity (after calcination). Sorbent size reduction below 10 μm dia. reflects a factor of 2 increase in sorbent utilization, whereas reduction below 2 μm dia. reflects a relatively minor explicit effect of particle size. This conclusion is supported by the results of Cole et al. (1986). However, the implicit effects of particle size (the effect of size on the surface area and porosity that evolve during calcination or hydration) may be much more important. Alterations in the pore size distribution play a very minor role in controlling sulfation, while increasing the sorbent porosity appears to be the single most promising way to enhance sulfation. This may be accomplished by choosing a high (15%) porosity carbonate or hydrate from which to derive the calcine.

Acknowledgment

This work was supported by Energy and Environmental Research Corporation and the U.S. Environmental Protection Agency under Contract No. 8562-1.

Literature Cited

- Cole, J. A., et al., "Fundamental Studies of Sorbent Reactivity in Isothermal Reactors," Joint EPA/EPRI Symp., Dry SO₂ Control. Raleigh, NC (June, 1986).
 Drehmel, D. C., "Limestone Injection Multistage Burner (LIMB). Status Report," Symp. FGD, New Orleans (Nov., 1983).
 Drehmel, D. C., G. B. Martin, and J. H. Abbott, "SO₂ Control with

- Limestone in Low-NO_x Systems: Development Status," *Proc. Symp. Flue Gas Desulfurization*, 2, EPRI CS-2897 (1983).
 Roman, V. P., L. J. Muzio, M. W. McElroy, K. W. Bowers, and D. T. Gallaspy, "Flow Reactor Study of Calcination and Sulfation," Paper No. 2B, 1st Joint EPRI/EPA Symp. on Dry SO₂ and Simultaneous SO₂/NO_x Control Technol., San Diego (1984).
 Simons, G. A., "The Physical Parameters Limiting Sulfation by CaO," SR-276, Physical Sciences Inc., Andover, MA (1987).
 Simons, G. A., and A. R. Garman, "Small Pore Closure and the Deactivation of the Limestone Sulfation Reaction," *AIChE J.*, 32, 1491 (1986).
 Simons, G. A., A. R. Garman, and A. A. Boni, "The Kinetic Rate of SO₂ Sorption by CaO," *AIChE J.*, 33, 211 (1987).

Manuscript received Jan. 20, 1987, and revision received June 10, 1987.

Errata

In the paper entitled "The Isothermal Flash Problem: New Methods for Phase Split Calculations" (33(6), p. 926, June 1987), we thank Dr. A. R. D. van Bergen for pointing out the revision of the Appendix.

$$f(\xi) = \left[\prod_{i=1}^N \left(\frac{z_i}{x_i y_i} - \xi \right) \right] \cdot \left[1 - \left(\sum_{i=1}^N \frac{1}{\frac{z_i}{x_i y_i} - \xi} \right) \right] = 0 \quad (\text{A2})$$

Ordering $\rho_i = (z_i/x_i y_i)$, $i = 1, \dots, N$ such that

$$0 < \rho_1 < \rho_2 < \dots < \rho_{N-1} < \rho_N \quad (\text{A3})$$

one can deduce that

$$f(\rho_i) = - \prod_{j \neq i}^N (\rho_j - \rho_i)$$

has the sign of $(-1)^i$, $i = 1, \dots, N$. Also,

$$f(0) = \left(\prod_{i=1}^N \frac{z_i}{x_i y_i} \right) \left(1 - \sum_{i=1}^N \frac{x_i y_i}{z_i} \right)$$

is strictly positive since Eq. A4 should be

$$0 < \xi_1 < \rho_1 < \xi_2 < \rho_2 < \dots < \xi_{N-1} < \rho_{N-1} < \xi_N < \rho_N \quad (\text{A4})$$

Therefore, all the eigenvalues of matrix \underline{A} are greater than 0, and \underline{A} is positively definite.

The final conclusion in the main demonstration remains valid and the only useful one.

Equation 10 should read:

$$\underline{A}^{-1} = VL \left[\frac{x_j y_j}{z_j} \left(\delta_{ij} + \frac{x_i y_i}{S} \right) \right]_{i,j=1,\dots,N} \quad (\text{10})$$

We would like to correct an error made in our R&D Note entitled "General Behavior of Dilute Binary Solutions" (Cochran and Lee, 1987) which extended the work of Debenedetti and Kumar (1986). The correct expression for our Eq. 6 should be:

$$K = [(G_{11}^\infty - G_{12}^\infty) + (G_{22}^\infty - G_{12}^\infty)] \rho. \quad (6)$$

Consequently, the correct expressions for our Eqs. 8, 9 and 10 should be:

$$K = \frac{n_{11}}{y_1} + \frac{n_{22}}{y_2} - \frac{2n_{12}}{y_1} - \rho(V_{11} + V_{22} - 2V_{12}) + \left(\frac{n_{11}^{LR}}{y_1} + \frac{n_{22}^{LR}}{y_2} - \frac{2n_{12}^{LR}}{y_1} \right) \quad (8)$$

$$K = \left[\frac{(\epsilon_{11}\sigma_{11}^3 + \epsilon_{22}\sigma_{22}^3 - 2\epsilon_{12}\sigma_{12}^3)}{\epsilon_{22}\sigma_{22}^3} \left(G_{22}^\infty + \frac{\pi}{6} \sigma_{22}^3 \right) - \frac{\pi(\sigma_{11}^3 + \sigma_{22}^3 - 2\sigma_{12}^3)}{6} \right] \rho \quad (9)$$

and

$$K = \frac{4\pi L_{22}^3}{3} \left[\frac{L_{11}^3}{L_{22}^3} \exp(-\lambda_{11}/kT) + \exp(-\lambda_{22}/kT) - \frac{2L_{12}^3}{L_{22}^3} \exp(-\lambda_{12}/kT) \right] - \frac{4\pi}{3} \rho(L_{11}^3 + L_{22}^3 - 2L_{12}^3) + G_{22}^\infty \rho \cdot \frac{(\lambda_{11}L_{11}^3 + \lambda_{22}L_{22}^3 - 2\lambda_{12}L_{12}^3)}{\lambda_{22}L_{22}^3}. \quad (10)$$

- Cochran, H. D., and L. L. Lee, "General Behavior of Dilute Binary Solutions," *AIChE J.*, 33(8), 1391 (Aug., 1987).
 Debenedetti, P. G., and S. K. Kumar, "Infinite Dilution Fugacity Coefficients and the General Behavior of Dilute Binary Systems," *AIChE J.*, 32(8), 1253 (Aug., 1986).

H. D. Cochran
 L. L. Lee